Metabolic behavior of hepatic VLDL and plasma LDL apoB-100 in African green monkeys

Carol A. Marzetta,[1,*] Fred L. Johnson,[*] Loren A. Zech,[†] David M. Foster,[**] and Lawrence L. Rudel[*]

Department of Comparative Medicine,[*] Bowman Gray School of Medicine of Wake Forest University, Winston-Salem, NC 27103; Laboratory of Mathematical Biology,[†] NCI, NIH, Bethesda, MD 20892; and Center for Bioengineering,[**] University of Washington, Seattle, WA 98195

Abstract Recently, evidence has accumulated suggesting that significant amounts of plasma low density lipoproteins (LDL) may be derived by direct production. These plasma very low density lipoprotein (VLDL)-independent sources include the production and secretion of LDL-like particles directly by the liver, and/or a small pool of nascent precursor particles that are converted rapidly to LDL. The current studies were designed to test the hypothesis that hepatic VLDL represent a rapidly turning over precursor pool to plasma LDL in African green monkeys. Livers from African green monkeys were perfused with serum-free medium containing [^{3}H]leucine or ^{3}H-labeled amino acids for 4–6 hr. Hepatic [^{3}H]VLDL and autologous plasma ^{125}I-labeled LDL were injected simultaneously into recipient animals and density gradient ultracentrifugation and gel filtration were used to characterize the distribution of ^{3}H and ^{125}I radioactivity at selected times after injection. These studies show that 4 to 66% of the injected dose of hepatic VLDL [^{3}H]apoB-100 was metabolized extremely rapidly into particles that resembled the recipient's plasma LDL by size and density. Based on the kinetic model developed to describe the metabolic behavior of hepatic VLDL [^{3}H]apoB-100, the estimated maximal pool size of hepatic VLDL apoB-100 in these animals was very small (0.042 and 0.112 mg) and represented, at best, approximately 10% of the average plasma VLDL apoB-100 mass found in cholesterol-fed African green monkeys. In addition, the radiolabeled hepatic LDL appear to be metabolized similarly to plasma LDL. That is, the rapid conversion of hepatic VLDL as well as the direct production of hepatic particles within the LDL density range appear to contribute to plasma LDL. Metabolic heterogeneity was also seen within the LDL class. The more buoyant subfraction (LDL_1) had a higher turnover rate than the more dense subfraction (LDL_2) and hepatic VLDL-derived [^{3}H]LDL_1 had a slower final rate of plasma disappearance than the plasma-derived ^{125}I-labeled LDL_1 in most animals. The results from these studies suggest that a small pool of hepatic VLDL can be converted very rapidly to plasma LDL and may contribute significantly to the large plasma pool of LDL seen in cholesterol-fed African green monkeys. This pathway may be analogous to the pathway in some human subjects in which a portion of human plasma VLDL is converted rapidly into LDL without passing through a delipidation cascade, often referred to as direct LDL production.—**Marzetta, C. A., F. L. Johnson, L. A. Zech, D. M. Foster, and L. L. Rudel.** Metabolic behavior of hepatic VLDL and plasma LDL apoB-100 in African green monkeys. *J. Lipid Res.* 1989. **30:** 357–370.

Supplementary key words apolipoprotein B • very low density lipoprotein • low density lipoprotein • hepatic lipoproteins

Plasma low density lipoproteins (LDL) are heterogeneous by size, density, composition, and metabolic behavior (1–8). Plasma triglyceride concentration, the intravascular environment, diet, and genotype are known to influence the physical characteristics, composition, and metabolic fate of LDL (9–11; Krauss, R. M., J. J. Albers, M. A. Austin, and J. D. Brunzell, unpublished observations). In addition to LDL differences seen among individuals, various kinds of LDL subfractions have been identified within an individual (1, 2, 4–7, 10). Although our knowledge about the complexities of LDL heterogeneity has advanced in recent years, the origin of different kinds of LDL is still poorly understood.

Turnover studies of plasma very low density lipoproteins (VLDL) have been used to estimate the contribution of VLDL apoB-100 to plasma LDL apoB-100. In normolipidemic subjects, 50–100% of all plasma LDL apoB-100 are thought to be derived from the catabolism of plasma VLDL (12, 13). In some types of hyperlipidemics, the amount of LDL apoB-100 derived from plasma VLDL-independent sources is much greater, suggesting that a

Abbreviations: d, density; DGUC, density gradient ultracentrifugation; DTNB, 5,5'-dithiobis-(2-nitrobenzoic acid); EDTA, ethelenediaminetetraacetic acid; FCR, fractional catabolic rate; LCAT, lecithin:cholesterol acyltransferase; LSS, least sum of squares; HDL, high density lipoproteins; NaN_3, sodium azide; P/S, polyunsaturated fat/saturated fat; SAA, serum amyloid apoprotein; SD, standard deviation; SDS-PAGGE, sodium dodecyl sulfate-polyacrylamide gradient gel electrophoresis; SS, sum of squares; VLDL, very low density lipoproteins; LDL, low density lipoproteins; IDL, intermediate density lipoproteins; LTP, lipid transfer protein; LpL, lipoprotein lipase.

[1]To whom correspondence should be addressed at present address: Department of Medicine, Division of Metabolism, Endocrinology and Nutrition, RG-26, University of Washington, Seattle, WA 98195.

Downloaded from www.jlr.org by guest, on June 19, 2012

major portion of plasma LDL is derived by direct production (12). Direct production of LDL can be defined as: *1*) LDL-like particles synthesized and secreted directly from the liver; and/or *2*) a small pool of nascent precursor particles that are converted very rapidly to LDL (13–15).

The direct production of LDL-like particles has been supported by liver perfusion studies done in a variety of animals (16–23). In these animals, a variety of apoB-containing lipoproteins is produced which can be isolated within the size and density ranges of plasma VLDL, IDL, and LDL. However, these hepatic lipoproteins differ in lipid and apolipoprotein composition from their plasma counterparts (19–23). Since apoB-100 does not exchange between particles and is the main apolipoprotein of LDL, all hepatic apoB-containing lipoproteins are potential precursors to plasma LDL.

Although it is unclear how similar or dissimilar human hepatic lipoproteins are to the various hepatic lipoproteins described in rats, rabbits, and monkeys, several laboratories (24–26) have shown that cultured Hep G2 cells (a transformed human hepatoma cell line) synthesize and secrete lipoproteins with some characteristics similar to those produced by perfused livers from African green monkeys (19, 20, 22). However, the extent to which comparisons should be made between lipoproteins produced by cultured Hep G2 cells versus perfused livers is unclear.

The contribution of a small rapidly turning over pool of precursor particles to plasma LDL has been suggested previously (13–15) but experimental evidence for this hypothesis is difficult to obtain. If these particles exist, they would be underrepresented among the more slowly metabolized precursor particles and would not be detected by conventional kinetic analyses. It is possible, however, to isolate nascent lipoproteins from perfused livers and examine their metabolic behavior in animal models.

Lipoprotein production by isolated perfused livers from African green monkeys has been well described (20, 21, 23) as well as the structural and metabolic characteristics of plasma LDL in this species (27, 28). Therefore, we chose the African green monkey as an animal model to test the hypothesis that hepatic VLDL isolated from perfused livers could represent a rapidly turning over precursor pool to plasma LDL.

MATERIAL AND METHODS

Animals and diets

All animals used for these studies were adult male African green monkeys (*Cercopithecus aethiops*). Each animal had been fed diets containing 0.8 mg of cholesterol/kcal in which 40% of total calories were from polyunsaturated fat (P/S ratio = 2.0; studies I, II, and III) or from saturated fat (P/S ratio = 0.3; studies IV, V, and VI) for at least 6 months prior to the start of these studies (29). Each study represents an individual recipient animal.

Preparation of recipient animals

At least 1 week prior to the start of a metabolic study, each recipient animal was given drinking water containing 0.05% NaI to prevent radioactivity iodide uptake by the thyroid. The animals were maintained on the NaI solution throughout the study. Each recipient animal was adapted to wearing a monkey jacket with a 2-ft tether line (Alice King Chatham, Inc., Los Angeles, CA) that attached to the back of the cage. Monkey jackets allowed the animals to be maintained in a relatively unrestricted, minimally stressful environment and avoided the need to repeatedly anesthetize the animals for the blood samples drawn during a study. Two days prior to surgery, each animal was given 400 mg/day of Cefadyl (Bristol Labs, Syracuse, NY) by intramuscular injection and 800 mg/day for the following 2 days. Before surgery, the animals were fasted overnight and immobilized with Ketamine (Parke-Davis, Morris Plains, NJ) throughout surgery. Sterilized tygon cannulas (0.03 in ID × 0.065 in OD; Dow Corning, Midland, MI) were surgically implanted into a femoral artery and vein. The cannulas were then threaded under the skin to the midback, out through the tether line, and out the back of the cage so that blood samples could be drawn without disturbing the animals. Immediately after surgery, saline was infused at the rate of 0.05 ml/min to maintain patent cannulas (Harvard Apparatus Compact Infusion Pump; Southnatick, MA). Radiolabeled lipoproteins were injected into recipient animals 3–5 days after surgery.

Liver perfusions

Liver perfusions were performed according to the method described by Johnson, St. Clair, and Rudel (19). A Krebs-Henseleit bicarbonate medium containing glucose, amino acids, insulin, cortisol, penicillin, streptomycin, and washed human erythrocytes was recirculated through each liver for 90 min. This medium was then removed and discarded, and fresh medium was recirculated through each liver for a second period of 4–6 hr. Ten mCi of ^{3}H-labeled amino acids [lysine, leucine, aspartate, glutamate, and glycine (New England Nuclear, Boston, MA) or lysine, leucine, phenylalanine, proline, and tyrosine (Amersham, Arlington Heights, IL)] or 10 mCi of [^{3}H]leucine (New England Nuclear) was added at the beginning of the second recirculating perfusion period. At the end of each experiment, the perfusate was collected on ice and 0.01% EDTA, 0.01% NaN_3, and 1 mM DTNB were added (final concentrations). Erythrocytes were removed by centrifugation at 2600 *g* for 30 min at 4°C. All livers were monitored for viability throughout the perfusion period based on periodic measurements of bile pro-

Downloaded from www.jlr.org by guest, on June 19, 2012

duction, oxygen consumption, cholesterol accumulation in the perfusate, and gross appearance of the liver.

Isolation and characterization of radiolabeled lipoproteins

Hepatic [^{3}H]VLDL (d < 1.006 g/ml) were isolated from perfusate by ultracentrifugation in a 60 Ti rotor at 50,000 rpm for 22 hr at 15°C. Each hepatic VLDL sample was concentrated to 2–3 ml by dialysis against 30% Dextran T-500 (Pharmacia) in distilled water containing 0.01% EDTA and 0.01% NaN_3. The concentrated samples were then dialyzed against 0.9% NaCl, 0.01% EDTA, and 0.01% NaN_3, pH 7.4. Three days prior to surgery, 5–7 ml of blood was drawn from each recipient animal. The d < 1.063 g/ml lipoproteins were isolated from plasma by ultracentrifugation and LDL were separated by gel filtration chromatography (30). Each LDL sample was concentrated in 30% dextran and then radiolabeled with ^{125}I by the method described by McFarlane (31) as modified by Bilheimer, Eisenberg, and Levy (32). Less than 1% of the radiolabel was TCA-soluble and greater than 91% was in apoB-100 as determined by SDS-PAGGE.

Radiolabeled lipoproteins were characterized by size using agarose column chromatography (30) and electron microscopy (19). Apoprotein composition and the distribution of radiolabel among the apoproteins were determined after separation of apoproteins by sodium dodecyl sulfate-polyacrylamide gradient gel electrophoresis (SDS-PAGGE) (27). After electrophoresis, each apoprotein band was sliced from the gel, cut into small pieces (~3 × 3 mm) and placed into uncapped 7-ml glass scintillation vials. Gel slices were dried in an 80°C oven for approximately 2 hr. Thirty percent H_2O_2 (200 μl) was then added to each vial and the vials were capped tightly and placed in a 70°C oven until the gels were completely digested (2–4 hr). The vials were removed from the oven and allowed to cool to room temperature. Five ml of Liquiscent (National Diagnostics, Somerville, NJ) was added to each vial and radioactivity was determined on a Beckman LS-7000 liquid scintillation counter. Radioactivity recovery from a representative study was 68.8 ± 8% (mean ± SD; n = 10).

Plasma and lipoprotein cholesterol (33), triglyceride (34), and protein (35) concentrations were measured as described previously. Bovine serum albumin (Fraction V, Sigma) was used as the protein standard. LDL protein as determined by the method of Lowry et al. (35) was assumed to be primarily apoB-100.

Design of the studies and lipoprotein characterizations

Hepatic lipoproteins were injected into recipient animals consuming the same diet as the liver donor animal. Each recipient animal was fasted overnight before receiving the injection of radiolabeled lipoproteins and remained without food until after the 6-hr blood sample. The animals were then fed their usual afternoon meal and returned to their normal feeding schedule throughout the remainder of the study (8:00 AM, after obtaining the blood sample, and 3:00 PM). In all but one study (III), autologous plasma ^{125}I-labeled LDL was injected simultaneously with hepatic [^{3}H]VLDL. Between 1.2 and 8.6 μCi of hepatic [^{3}H]apoB-100 and 0.23 and 5.4 μCi of plasma LDL ^{125}I-labeled apoB-100 was injected into each animal. The radiolabeled lipoproteins were injected into the venous cannula of the recipient monkey and flushed immediately with 3 ml of saline. Subsequent blood samples were drawn into sterile syringes from the arterial cannula and placed immediately on ice in tubes containing 1 mg/ml EDTA, 1 mg/ml NaN_3, and 0.4 mg/ml DTNB (final concentrations). Blood samples were taken 5 min before the start of the study, and then at 5, 15, 45, and 90 min, and 3, 6, 14, 24 hr, and then daily for up to 3 days after injecting the radiolabeled lipoproteins. Aliquots of each plasma sample were added to 7-ml glass scintillation vials with 3 ml of Liquiscint added to each vial. The radioactivity in each vial was measured using a TM Analytic Gamma Counter (Elk Grove Village, IL) and a Beckman LS-7000 liquid scintillation counter programmed for double-isotope counting using the automatic quench correction. All samples were corrected for background radioactivity, quench, and ^{125}I radioactivity in the tritium window.

To isolate apoB-containing lipoproteins, the density of each plasma sample (2 ml) was raised to 1.080 g/ml with solid KBr. Each sample was then poured into a Beckman 13-ml polyallomer ultracentrifuge tube, overlayered with a d 1.080 g/ml solution, and ultracentrifuged in an SW-40 rotor at 40,000 rpm for 24 hr at 15°C. The percentage of ^{3}H and ^{125}I radioactivity recovered at this step from a representative study was 87.6 ± 7 and 93.3 ± 5, respectively (mean ± SD; n = 10 each). The lipoproteins that floated to the top of the tube were isolated by tube slicing, aliquots were taken to determine total protein (35), total radioactivity, and distribution of radioactivity among the apoproteins (SDS-PAGGE).

The density distribution of the radiolabeled lipoproteins was determined by density gradient ultracentrifugation (DGUC). The density of each sample was adjusted by dialysis 10 1.030 g/ml. For the injected material, an aliquot of the radiolabeled lipoproteins was added to the d < 1.080 g/ml lipoproteins from the blood sample taken prior to the start of the study. Discontinuous salt gradients were set up in Beckman 14-ml polyallomer ultracentrifuge tubes by first adding 4.5 ml of a d 1.006 g/ml solution and then successively underlayering 5.5 ml of a d 1.030 g/ml solution (containing the lipoprotein sample) and 4 ml of a d 1.050 g/ml solution. All density solutions were made by adding solid KBr to 0.9% NaCl

Downloaded from www.jlr.org by guest, on June 19, 2012

containing 0.01% EDTA and 0.01% NaN_3. A tube containing the same density solutions but without the lipoprotein sample was prepared at the same time. Ultracentrifugation was done in an SW-40 rotor at 40,000 rpm for 24 hr at 20°C and samples were drained from the ultracentrifuge tubes as described previously (27). An aliquot was taken from each fraction to determine the distribution of radioactivity by density. The percentage of ^3H and ^{125}I radioactivity recovered at this step in a representative study was 88.2 ± 6 and 88.8 ± 6, respectively (mean ± SD; n = 9 each). The refractive index (ABBE-3L Refractometer; Bausch and Lomb, Rochester, NY) was measured on alternate fractions collected from the blank tubes at 20°C. The density of each solution was determined using standard solutions of known densities and their refractive indexes. Based on the DGUC profiles of each animal, radioactivity within each specific density range (VLDL-IDL, LDL_1, and LDL_2) was summed. Since the percentage of radiolabel in LDL apoB-100 based on SDS-PAGGE was generally greater than 90% (89 ± 8% and 93 ± 2%, mean ± SD for ^3H- and ^{125}I-radiolabeled lipoproteins, respectively) after injection, the total radioactivity in LDL was assumed to be primarily apoB-100.

Model development and testing

The data were analyzed by compartmental modeling using the SAAM 29/CON 29 simulator on a DEC VAX 11/730 computer system (36, 37). Plasma volumes were assumed to be 3.5% of body weight. Statistical analyses on differences between the terminal slopes of the plasma disappearance curves were done using the comparison of regression lines test of Snedecor and Cochran (38).

The initial conditions (injected radioactivity) of the hepatic ^3H-labeled lipoproteins were distributed among the VLDL-IDL, LDL_1, and LDL_2 density ranges according to the DGUC profiles of the injected ^3H-labeled hepatic lipoprotein preparations. These radiolabeled lipoproteins represent "nascent" hepatic particles with physical and chemical characteristics distinct from their plasma counterparts (19, 20, 22) and, therefore, were assigned to hepatic lipoprotein metabolic pools (hVLDL, $hLDL_1$, and $hLDL_2$). After 5 min (the first plasma time point), the ^3H radioactivity was considered a part of, and indistinguishable from, plasma lipoprotein pools. The fractional rates of irreversible loss of hVLDL, $hLDL_1$, and $hLDL_2$ were estimated based on the amount of the injected radioactivity not needed to account for the radioactivity in the plasma lipoprotein pools for VLDL-IDL, LDL_1, and LDL_2 at the 5-min time point. These exit rates were assumed to be the same for hVLDL, $hLDL_1$, and $hLDL_2$ since the relative ratio of apoE to apoB-100, the primary ligands for receptor binding, is similar in both hepatic VLDL and LDL (20). When these rates were allowed to adjust, all exit rates were within 10% of the fixed rates but undefined in two out of the six animals. The turnover rates of hVLDL, $hLDL_1$, and $hLDL_2$ were extremely rapid. Based on sensitivity plot analyses (total sums of squares/least sums of squares), the turnover rates of the hepatic lipoproteins were set to 50 pools/hr for all final calculations. The fraction of each hepatic lipoprotein subpopulation (hVLDL, $hLDL_1$, and $hLDL_2$) was distributed to plasma VLDL-IDL, LDL_1, and LDL_2 and adjusted independently for each animal based on the observed data.

An extravascular pool was assumed not to exist for VLDL-IDL because of the relatively large size of these particles. An extravascular pool was tested for all LDL_1 dieaway curves and fit the data equally well. However, with an extravascular pool the decay of particles in LDL_1 was very fast compared to the plasma-derived LDL_1 and LDL_2. Therefore, a slowly turning over second pool rather than an extravascular pool was added to the LDL_1 portion of the model. An extravascular pool was assumed to exist in the LDL_2 portion of the model; however, large fractional standard deviations (FSDs > 150%) were associated with these rates. Therefore, the pathways between the intra- and extravascular pools were not included in the final analyses.

A direct pathway between hepatic VLDL and plasma LDL_1 or LDL_2 was required for each animal to account for the rapid appearance of [^3H]apoB-100 radioactivity in the LDL density range. Although a pathway between hepatic VLDL and LDL_1 could not be differentiated from a pathway between hepatic VLDL and LDL_2, one of these pathways was absolutely required for each animal. When both of these pathways were included in the model, neither one could be determined with any degree of certainty (FSDs > 100%); therefore, hepatic VLDL radioactivity was distributed to LDL_1 only. For radiolabeled hepatic LDL, it was assumed that hepatic LDL_1 could contribute directly to LDL_2 but that hepatic LDL_2 could not contribute directly to the more buoyant LDL_1 particles. For the final iterations, all fractional standard deviations were less than 65%, most being less than 30%.

The calculated sizes of the hVLDL, $hLDL_1$, and $hLDL_2$ were estimated by assuming that the hepatic lipoproteins were the sole source of the LDL_1 plus LDL_2 apoB-100 pool and assuming the distribution of radioactivity and mass were the same among the hepatic lipoproteins in the injected material. Therefore, these estimates represent maximal pool sizes for the hepatic lipoproteins.

RESULTS

Table 1 shows the average plasma cholesterol and lipoprotein cholesterol concentrations of each recipient animal. Total plasma cholesterol (TPC) and triglyceride (TG) concentrations ranged from 160 to 593 mg/dl and 6 to 44 mg/dl, respectively. The variability in TPC response

Downloaded from www.jlr.org by guest, on June 19, 2012

TABLE 1. Total plasma cholesterol, triglyceride, and lipoprotein cholesterol concentrations

Study	Animal	Diet	Plasma Concentrations[a] TPC[b]	TG[b]	VLDL + IDL[c]	LDL[c]	HDL[b]
					mg/dl		
I	201	PUS	474	12	28	417	29
II	223	PUS	310	14	19	275	16
III	241	PUS	289	6	17	248	24
IV	298	SAT	160	26	10	72	78
V	304	SAT	460	21	28	384	48
VI	306	SAT	593	44	36	483	74

[a]TPC, total plasma cholesterol; TG, total plasma triglyceride; lipoproteins separated by agarose column chromatography (31). VLDL + IDL, very low density lipoprotein and intermediate density lipoprotein cholesterol (regions I and II from agarose column chromatography, ref. 25); LDL, low density lipoprotein cholesterol; HDL, high density lipoprotein cholesterol; PUS, polyunsaturated fat; SAT, saturated fat.
[b]Average of 4–8 determinations.
[c]Calculated from the average percentage cholesterol distribution determined on animals 201, 241, and 306.

to dietary cholesterol in these animals is characteristic of larger groups of cholesterol-fed African green monkeys. No consistent differences in TPC or lipoprotein cholesterol distribution were seen between the polyunsaturated (PUS) and saturated (SAT) fat-fed animals. On the average, plasma TG was lower in the PUS fat-fed animals than in the SAT fat-fed animals (11 ± 4 vs. 30 ± 12 mg/dl, respectively).

A representative electron micrograph of a radiolabeled hepatic lipoprotein preparation and the average size distribution of all the hepatic lipoprotein preparations as determined by electron microscopy is shown in **Fig. 1.** The hepatic lipoproteins were generally round in appearance, although excess surface material was seen on some particles (arrows). These particles varied from 175 to 625 Å in diameter and were skewed slightly in their distribution with a mean diameter of 327 Å and a median diameter of 385 Å. **Fig. 2** shows a selected SDS-PAGGE pattern of a hepatic lipoprotein preparation. ApoB-100 was the major apoprotein but variable amounts of apoE, Cs, A-II, and SAA were also seen. On the average, 73% (53 to 89%) of the total radioactivity was isolated with apoB-100, 9% (3 to 17%) with apoE, and 18% (7 to 25%) with apoA-II, Cs, and SAA. ApoB-48 was not detected by SDS-PAGGE in any sample.

Five minutes after injection of the radiolabeled lipoproteins, 89 ± 8% and 93 ± 2% (mean ± SD) of the ^{3}H and ^{125}I radioactivity, respectively, in the d < 1.080 g/ml lipoproteins was associated with apoB-100 as determined by SDS-PAGGE. **Fig. 3** illustrates the appearance of hepatic lipoprotein-derived ^{3}H radioactivity into particles within the LDL density and size range in a representative animal (study II). Five minutes after injection of the radiolabeled lipoproteins, 76.5% of the ^{3}H radioactivity was isolated within the LDL_1 and LDL_2 (Fig. 3, left panels). The distribution of ^{125}I-labeled LDL radioactivity was superimposable with the distribution of LDL protein mass in each animal (data not shown). Within 45 min, the density distribution of hepatic VLDL ^{3}H radioactivity resembled the heterogeneous distribution of the recipient animal's plasma ^{125}I-labeled LDL. Concomitantly, as the density increased, the average size of the hepatic VLDL-derived [^{3}H]apoB-100 particles decreased and resembled the size distribution of the plasma ^{125}I-labeled LDL of the recipient animal as determined by gel filtration chromatography (Fig. 3, right panels). This rapid conversion of hepatic VLDL to plasma LDL was seen in five of the six animals studied. In the sixth animal (study VI), the conversion of hepatic VLDL-derived ^{3}H radioactivity to particles with the distribution of the recipient animal's LDL took approximately 2 hr.

Radioactivity isolated within the VLDL-IDL, LDL_1, and LDL_2 density ranges based on DGUC was summed and plotted against time for each animal. **Fig. 4** shows the ^{3}H-labeled and ^{125}I-labeled apoB-100 plasma disappearance curves of each density subfraction in three different animals. The density ranges for the LDL subfractions for each animal were chosen empirically based on the appearance of lipoprotein density heterogeneity. In all studies, hepatic VLDL [^{3}H]apoB-100 radioactivity disappeared rapidly from the VLDL-IDL density range without any initial flatness or delay such as that associated with a delipidation cascade described for human VLDL apoB-100. After the initial rapid disappearance, the apoB-containing particles remaining in the VLDL-IDL density range were cleared at a much slower rate. The metabolism of ^{125}I-labeled and [^{3}H]apoB-100 from the LDL_1 density range was biexponential in all studies. The rates of disappearance of the final slope of hepatic ^{3}H-derived and plasma ^{125}I-derived apoB-100 radioactivity in the LDL_1 density range were the same in study V (0.033 vs. 0.033 hr^{-1}). This is in contrast to the slower clearance rates of

Downloaded from www.jlr.org by guest, on June 19, 2012

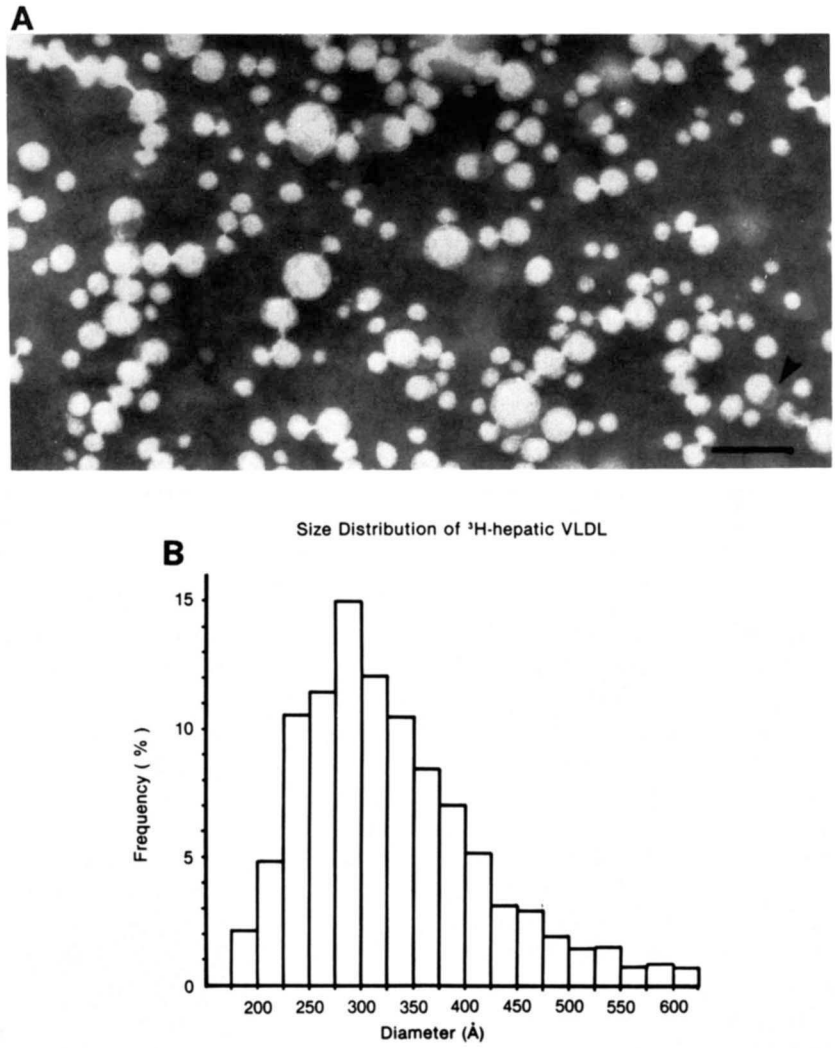

Fig. 1. A: An electron micrograph of a negative-stained, radiolabeled hepatic lipoprotein preparation (studies VI and V). In general, the particles are spherical and heterogeneous in size, ranging from 175 to 624 Å in diameter. In each preparation, some excess was seen on some particles (arrows). B: The size distribution of all the radiolabeled hepatic VLDL preparations (n = 4). The diameters of 300–400 particles were measured for each hepatic lipoprotein preparation. Total magnification was × 144,200; bar marker represents 1000 Å.

the final slope of hepatic ^{3}H-derived and plasma ^{125}I-derived apoB-100 LDL_1 radioactivity in studies II and VI (0.027 vs. 0.038 hr^{-1} and 0.015 vs. 0.029 hr^{-1}, respectively; $P < 0.001$; see Fig. 4). The final disappearance of hepatic lipoprotein-derived LDL_1 apoB-100 had a slower rate of clearance than the plasma ^{125}I-labeled LDL in three of five animals studied and could not be accounted for by the input of radioactivity from VLDL-IDL (pool 1). The [^{3}H]apoB-100 radioactivity in the LDL_2 density range increased initially and then disappeared monoexponentially while the ^{125}I-labeled apoB-100 disappeared monoexponentially in most animals. In addition, the final exponential of the ^{3}H-labeled and ^{125}I-labeled apoB-100 disappearance curves of the LDL_2 subfraction had the same or similar clearance rates (0.021 vs. 0.023 hr^{-1}; 0.024 vs. 0.022 hr^{-1}, and 0.006 vs. 0.007 hr^{-1} for studies II, V, and VI, respectively; see Fig. 4).

The compartmental model developed to help explain the metabolic behavior of the ^{3}H-labeled hepatic lipoproteins is shown in **Fig. 5.** The rate constants for each parameter and the estimated pool sizes for each compartment are given in **Table 2.** Conceptually, the hepatic lipoprotein metabolic pools represent the nascent hepatic particles that were injected into each animal. These lipoproteins have been modified minimally by most intravascular enzymes and differ morphologically and chemically from their plasma counterparts.

The VLDL-IDL density range could be described by two compartments. Pool 11 had a slow turnover rate compared to pool 1. Based on the calculated pool sizes derived

Downloaded from www.jlr.org by guest, on June 19, 2012

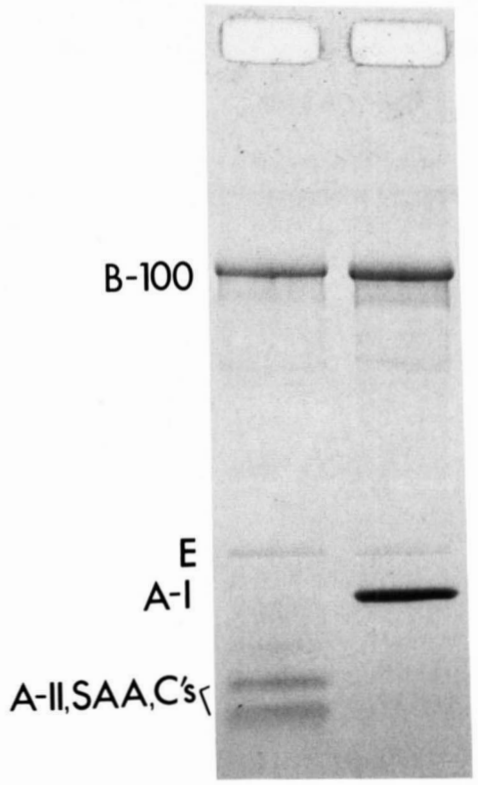

Fig. 2. A representative 4–30% SDS-PAGGE of a hepatic lipoprotein preparation (study III). Approximately 30 μg of protein was added to each well. After electrophoresis, the gel was stained with Coomassie blue. The left lane shows the distribution of apoproteins B-100, E, A-I, and small apoproteins A-II, SAA, and Cs of the hepatic lipoprotein sample. The right lane is the apoprotein distribution of plasma d < 1.21 g/ml lipoproteins from an African green monkey for comparison.

from the model, the slowly turning over pool (pool 11) contained 58–97% of the apoB-100 mass isolated in the VLDL-IDL density fraction.

The LDL_1 subfraction could also be described by two compartments, pool 2 and pool 12. Pool 12 is a slowly turning over pool relative to pool 2 and contained between 69 and 98% of the mass as determined by the model.

Between 5 and 52% of the [^{3}H]apoB-100 in pool 2 contributed to pool 3. The possibility of pathways from the slowly turning over pools of VLDL-IDL and LDL_1 (pools 11 and 12) to LDL_1 and/or LDL_2 were tested for all studies; however, in all animals these pathways were poorly defined (FSDs > 150%), and the early increase in ^{3}H radioactivity in LDL_2 could not be accounted for when these pathways were included.

The disappearance of [^{3}H]apoB-100 from the LDL_2 subfraction could be described by an intravascular and extravascular compartment. However, large standard deviations (FSDs > 150%) were associated with the rates between pool 3 and the extravascular pool (Fig. 5, unlabeled pool), and therefore, these pathways were not included in the final analyses.

To estimate the pool size of hepatic VLDL, LDL_1, and LDL_2 apoB-100, we assumed that these hepatic lipoproteins were the sole source of the plasma LDL apoB-100. These estimates, therefore, represent maximum hepatic lipoprotein apoB-100 pool sizes and ranged from 42 to 112 μg for hepatic VLDL, 26 to 50 μg for hepatic LDL_1, and 6 to 22 μg for hepatic LDL_2 (Table 2, M(hVLDL), M(hLDL_1), and M(hLDL_2), respectively).

Although the upper limits of these turnover rates could not be resolved from these data, sensitivity plots were calculated for each study in which the total sums of squares were divided by the least sums of squares to determine the turnover rate which would minimize the variance between the observed data and the best fit generated by the model (**Fig. 6**). In all studies, the turnover rates were estimated to be large (10–100 pools/hr). A more accurate estimate of these rates would require additional blood samples to be taken earlier than the first sample obtained in the current studies (5 min after injection).

DISCUSSION

The studies presented here have shown that within minutes, radiolabeled hepatic VLDL are metabolized rapidly to particles that resemble the size, density, and characteristic heterogeneity of each recipient animal's LDL. Based on the kinetic model developed to describe these data, between 4 to 66% of the injected dose of hepatic [^{3}H]VLDL was converted very rapidly to particles within the LDL density range. Assuming all plasma LDL are derived from the injected radiolabeled hepatic lipoproteins, 15 to 94% of the production rates of plasma LDL are derived from the direct conversion of hepatic VLDL to LDL [L(2,10)]. These are considered to be maximal estimates since other potential sources of plasma LDL exist.

The observations made in the current studies support recent experiments done by Goldberg et al. (15, 39). In their studies, up to 75% of plasma LDL in monkey chow-fed cynomolgus monkeys was suggested to be derived via direct production. However, during acute lipoprotein lipase inhibition, direct production of LDL independent of the VLDL delipidation cascade could not be demonstrated, suggesting the rapid conversion of a portion of VLDL to LDL in these animals.

Several studies in humans (13, 40–43), nonhuman primates (39, 44, 45), miniature pigs (46), and rats (47) have suggested that not all plasma LDL are derived from the catabolism of plasma VLDL, implicating the direct production of LDL from the liver. It is unclear, however, whether a portion of plasma LDL is synthesized and secreted by the liver directly and/or whether a small pool of VLDL or IDL precursors is converted rapidly to plasma LDL (13–15). The present studies provide evi-

Downloaded from www.jlr.org by guest, on June 19, 2012

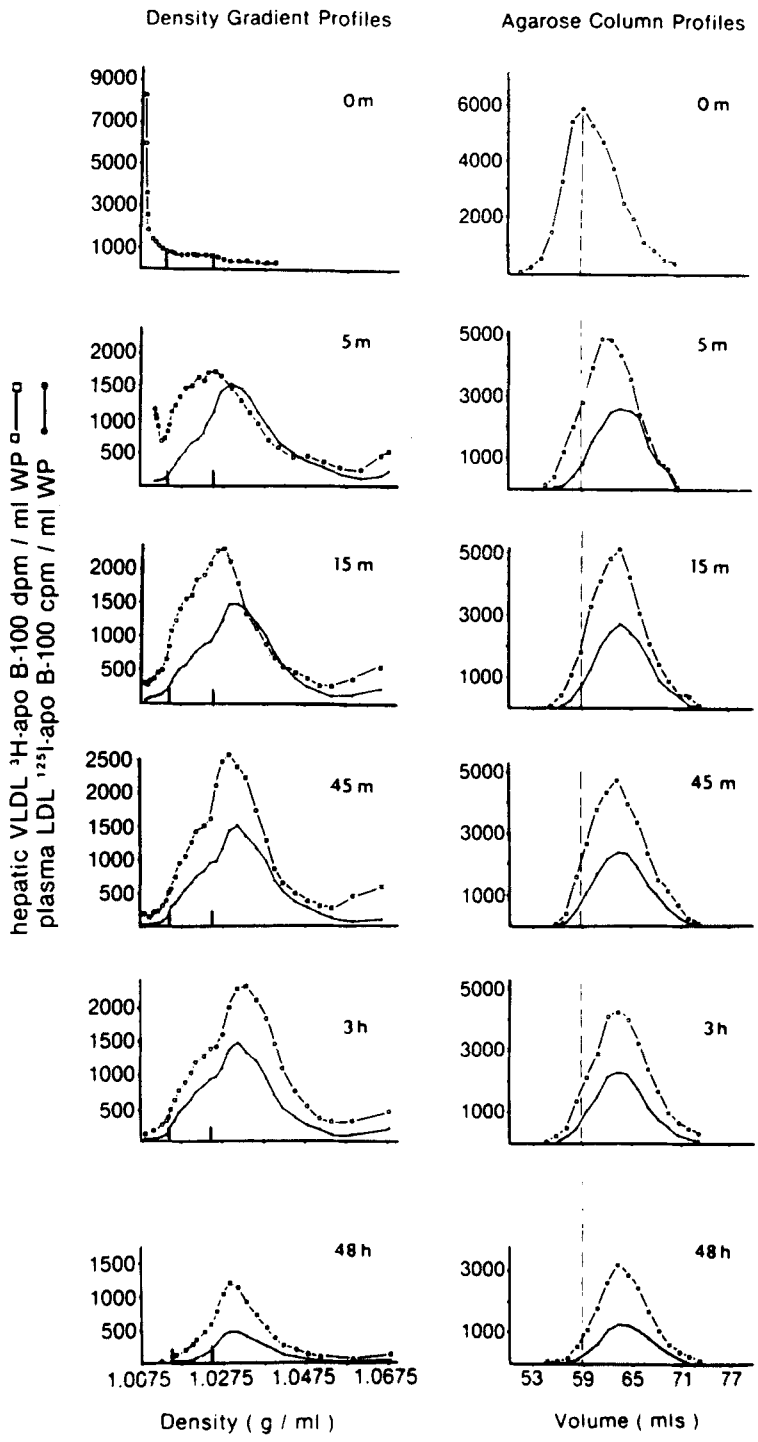

Fig. 3. Density gradient ultracentrifugation profiles (left panels) and agarose column elution profiles (right panels) of hepatic lipoprotein-derived radioactivity (□) and plasma LDL-derived radioactivity (●) of samples taken at selected times after injection of the radiolabeled lipoproteins (study II). The time given for each profile represents the time after the injection of the radiolabeled lipoproteins; m, minutes, h, hours. For the 0 m sample (the starting injected material), an aliquot of the radiolabeled lipoproteins was added to an aliquot of $d < 1.080$ g/ml lipoproteins isolated from whole plasma obtained from the recipient animal 5 min prior to the start of the study. The sample was then characterized by DGUC along with the other samples. The vertical lines on the DGUC profiles indicate the VLDL-IDL, LDL_1, and LDL_2 density cuts used in subsequent analyses. The vertical line on the agarose column profiles marks the average size of the injected hepatic ^3H-labeled lipoprotein. The % of injected dose in LDL_1 and LDL_2 for the DGUC profiles are: 0 m, 26.5% and 6.1%; 5 m, 41.7% and 34.8%; 15 m, 36.4% and 42.4%; 45 m, 25.4% and 51.1%; 3 h, 21.3% and 53.5%; and 48 h, 6.2% and 21.5%, respectively.

Downloaded from www.jlr.org by guest, on June 19, 2012

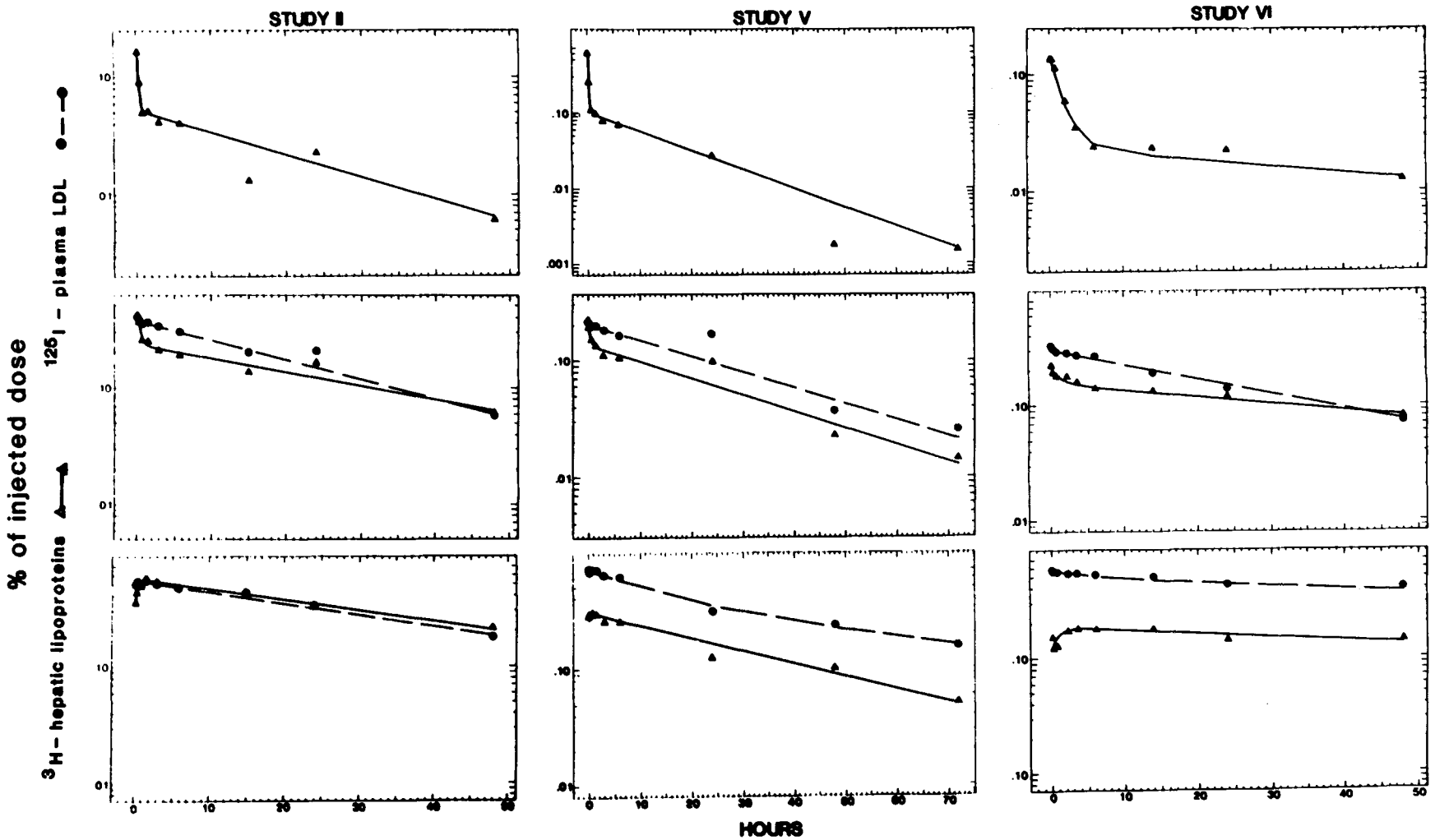

Fig. 4. The appearance and disappearance of hepatic lipoprotein-derived [^{3}H]apoB-100 particles (△) and plasma LDL-derived ^{125}I-labeled apoB-100 particles (●) with time after injection. The data points represent the observed data and the lines are the best fit generated by the kinetic model. For study II, the density ranges used were VLDL-IDL, d < 1.013 g/ml; LDL_1, 1.013 < d < 1.026 g/ml; and LDL_2, d > 1.026 g/ml. For study V, the density ranges used for these analyses were VLDL-IDL, d < 1.013 g/ml; LDL_1, 1.013 < d < 1.021 g/ml; and LDL_2, d > 1.021 g/ml. For study VI, the density ranges used were VLDL-IDL, d < 1.011 g/ml; LDL_1, 1.011 < d < 1.020 g/ml; and LDL_2, d > 1.020 g/ml.

Downloaded from www.jlr.org by guest, on June 19, 2012

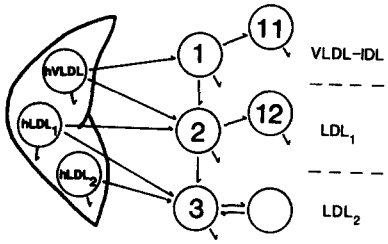

Fig. 5. The kinetic model describing the metabolic behavior of hepatic lipoprotein ^3H radioactivity. Pool 10 represents a very rapidly turning over pool of nascent hepatic VLDL that contributes to pools 1, 2, and 3 directly. Radiolabeled hepatic VLDL, LDL_1, and LDL_2 pools are represented by hVLDL, $hLDL_1$, and $hLDL_2$, respectively. Pools 1 and 11 represent plasma pools from the VLDL-IDL density range. Pool 11 is a slowly turning over pool compared to pool 1. Pools 2 and 12 represent the plasma pools from the LDL_1 density range. Pool 12 is a slowly turning over pool compared to pool 2. Pool 3 represents the plasma pool from the LDL_2 density range. The additional pool in LDL_2 (unlabeled) represents an extravascular pool.

dence to support the latter hypothesis and suggest that a pool of nascent hepatic VLDL can be converted very quickly to plasma LDL.

Based on the kinetic model, the predicted maximal apoB-100 pool size of the hepatic VLDL was between 42 and 112 μg which is approximately 5–12% of the average plasma VLDL apoB-100 mass found in cholesterol-fed African green monkeys (Wilson, M. D. and L. L. Rudel, unpublished observations). This maximal pool size is based on the assumption that all LDL apoB-100 are derived from injected radiolabeled hepatic lipoproteins and therefore are assumed to represent an overestimation. However, even using the maximal estimates of the hepatic VLDL apoB-100 pool size, these nascent lipoproteins would be undetectable and indistinguishable from the other d < 1.006 g/ml lipoproteins isolated from plasma based on current methodology.

In three out of five animals in which lipoprotein pool sizes have been estimated by the model, the predicted pool size of plasma VLDL (M(1) + M(11); Table 2) is 5–9 times greater than the VLDL apoB pool size in other cholesterol-fed African green monkeys. Although we have assumed that no extravascular pool exists for VLDL, perhaps this is naive. Although the estimated plasma

TABLE 2. Estimated rate constants (hr^{-1}) and apoB-100 pool sizes (mg) for all studies[a]

Parameter	Study I	II	III	IV	V	VI	Mean ± SD
IC(hVLDL)[b]	0.681	0.674	0.811	0.500	0.500	0.590	0.626 (.120)
IC($hLDL_1$)	0.263	0.265	0.161	0.347	0.247	0.305	0.265 (.062)
IC($hLDL_2$)	0.056	0.061	0.028	0.153	0.153	0.105	0.093 (.053)
L(0,hVLDL)[c]	0.319	0	0.640	0.474	0.391	0.510	0.389 (.220)
L(1,hVLDL)	0.312	0.339	0.316	0.208	0.181	0.268	0.271 (.069)
L(2,hVLDL)	0.369	0.661	0.044	0.318	0.428	0.222	0.340 (.207)
L(0,$hLDL_1$)	0.319	0	0.640	0.474	0.391	0.510	0.389 (.220)
L(2,$hLDL_1$)	0.152	0.029	0.298	0.119	0.085	0.253	0.150 (.108)
L(3,$hLDL_1$)	0.529	0.971	0.062	0.407	0.523	0.237	0.461 (.312)
L(0,$hLDL_2$)	0.319	0	0.640	0.474	0.391	0.510	0.389 (.220)
L(3,$hLDL_2$)	0.681	1.00	0.360	0.526	0.609	0.490	0.611 (.220)
L(0,1)	2.84 (.500)	4.54 (.756)	0.193 (.066)	1.33 (.066)	4.21 (.787)	0.515 (.062)	1.67 (1.70)
L(2,1)	0.415 (.072)	0.675 (.010)	0.896 (.176)	0.153 (.008)	2.17 (.358)	0.070 (.009)	1.33 (2.21)
L(11,1)	0.893 (.177)	1.54 (.219)	0.405 (.081)	0.045 (.005)	0.866 (.107)	0.119 (.027)	0.645 (.567)
L(0,11)	0.078 (.005)	0.044 (.002)	0.049 (0)	0.033 (.003)	0.080 (.002)	0.015 (.003)	0.050 (.025)
L(0,2)	0	0	0.092 (.017)	0.348 (.065)	1.47 (.582)	0	0.425 (.836)
L(3,2)	0.635 (.273)	1.38 (.052)	0.214 (.040)	0.039 (.007)	0.163 (.065)	0.191 (.077)	0.410 (.526)
L(12,2)	0.920 (.447)	1.29 (.432)	0.399 (.098)	0.169 (.052)	1.55 (.587)	0.512 (.366)	0.820 (.563)
L(0,12)	0.028 (.006)	0.027 (.002)	0.036[d]	0.075 (.004)	0.033 (.002)	0.015 (.003)	0.036 (.021)
L(0,3)	0.021 (.005)	0.021 (.002)	0.024[d]	0.049 (.002)	0.024 (.001)	0.006 (.003)	0.024 (.014)
M(hVLDL)	0.112 (.014)	0.067 (.005)		0.042 (.001)	0.072 (.003)	0.052 (.016)	0.069 (.027)
M($hLDL_1$)	0.043 (.006)	0.026 (.002)		0.029 (.001)	0.050 (.002)	0.027 (.008)	0.035 (.011)
M($hLDL_2$)	0.009 (.001)	0.006 (.0004)		0.013 (.0004)	0.022 (.001)	0.009 (.003)	0.012 (.006)
M(1)	0.423 (.082)	0.167 (.031)		0.286 (.017)	0.090 (.010)	0.997 (.334)	0.393 (.361)
M(11)	4.82 (.646)	5.93 (.485)		0.392 (.029)	0.967 (.055)	7.85 (2.63)	3.99 (3.22)
M(2)	1.66 (.768)	0.884 (.279)		1.60 (.321)	0.584 (.267)	1.41 (1.90)	1.23 (.472)
M(12)	55.34 (9.90)	42.48 (3.60)		3.60 (.352)	29.10 (1.40)	47.39 (15.7)	35.58 (20.26)
M(3)	120.10 (10.33)	132.34 (3.66)		20.40 (.271)	84.42 (1.35)	128.30 (17.1)	97.11 (46.87)

[a]Animals from studies I and II were injected with hepatic lipoprotein preparation no. 1; ;animals from studies IV and V were injected with prep no. 2; and animals from studies III and VI were injected with preps no. 3 and no. 4, respectively.

[b]ICs represent the initial conditions given as percent of distribution of injectate radioactivity among the hepatic lipoproteins.

[c]All rates from the hVLDL, hLDL, $hLDL_1$, and $hLDL_2$ pools are given as percentages. Ls represent rate constants and Ms represent mass as described previously (37). Numbers in parentheses are the standard deviations for each rate constant.

[d]Study III was carried out to 14 hr after the injection of the radiolabeled lipoproteins; therefore L(0,12) and L(0,3) were fixed to the average rate of these parameters determined from the other studies. LDL apoB mass was not determined for Study III.

Downloaded from www.jlr.org by guest, on June 19, 2012

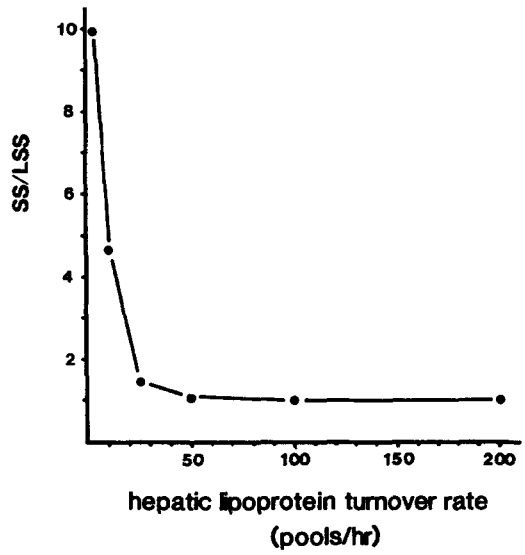

Fig. 6. A sensitivity plot from a representative animal (study VI) showing the relationship between the total sum of squares (SS) divided by the least sum of squares (LSS) and the rate at which hVLDL, $hLDL_1$, and $hLDL_2$ turn over. The variance between the observed data and the best fit generated by the model is the lowest (approximately 1.0) when the turnover rates are equal to 50 pool hr^{-1} and increases rapidly when these rates are less than 50 pool hr^{-1}.

VLDL pool sizes for studies IV and V are within a physiological range, accurate estimates of these metabolic pools would require actual measurements of plasma VLDL apoB which were unavailable at the time of these studies.

The conventional metabolic pathways characterizing the conversion of human plasma VLDL to IDL and LDL were not compatible with the data obtained from the current studies for a number of reasons. First, the appearance of hepatic [^{3}H]VLDL in the LDL density range was much more rapid (minutes) than is typically seen for plasma VLDL (hours); therefore, a direct pathway from hepatic VLDL to LDL was required to fit the observed data. Second, the disappearance of hepatic ^{3}H radioactivity from the VLDL-IDL density range was very rapid, without any delay or shoulder which is characteristic of a delipidation cascade (13). Therefore, only a rapidly turning over pool, to account for the initial rapid loss of radiolabeled particles, and a single more slowly turning over pool, to account for the tail portion, were needed to describe the disappearance of ^{3}H radioactivity from the VLDL-IDL density range. Finally, a simple two-pool LDL model was not compatible with the observed data. Two LDL density subfractions were characteristic among most of the animals (see Fig. 3); therefore, we assigned a metabolic pool to the buoyant and the dense LDL subfractions (LDL_1 and LDL_2, respectively). As described previously, an additional slowly turning over pool was required for LDL_1 while an extravascular pool (although not well defined) was included for LDL_2.

Several models were tested to account for the rapid appearance of ^{3}H radioactivity in LDL_1 and LDL_2. First, the initial conditions (injected ^{3}H radioactivity) were assigned to a plasma VLDL-IDL pool, which was then distributed to LDL_1 and LDL_2 pools. However, the radioactivity in the early time points in LDL_1 and LDL_2 could not be accounted for, even when 100% of the radioactivity in VLDL-IDL was sent to LDL_1 and then to LDL_2. Second, initial conditions were assigned to VLDL-IDL, LDL_1, and LDL_2 pools as defined by the density distribution of radiolabel of the injected hepatic lipoprotein. When this was done two additional pools, one in VLDL-IDL and one in LDL_2, had to be added to the model to fit the data adequately. The added pool in the VLDL-IDL subfraction had to contribute directly to LDL_1 and LDL_2 and turn over very rapidly. In addition, the initial conditions in pools 2 and 3 predicted by this model were twice as high as the observed ^{3}H radioactivity. Therefore, the model was modified to include hepatic lipoprotein pools of VLDL, LDL_1, and LDL_2 which contribute rapidly to the plasma VLDL-IDL, LDL_1, and LDL_2 pools.

The metabolic behavior of plasma VLDL has not been described in African green monkeys. However, Goldberg et al. (39) have studied the metabolic behavior of plasma VLDL and LDL apoB-100 using sequential ultracentrifugation in monkey chow-fed cynomolgus monkeys. In their studies, the conversion of plasma VLDL to LDL was relatively slow (approximately 2 hr) compared to the rapid conversion (minutes) of hepatic VLDL to plasma LDL seen in the studies presented here, although it is unclear how directly comparisons can be made between these two studies.

The mechanism by which hepatic VLDL is converted rapidly to LDL is unknown. African green monkey hepatic VLDL are rich in triglyceride and phospholipid and represent nascent-like particles that have been unaffected by the major intravascular enzymes (lipoprotein lipase [LpL], lipid transfer protein [LTP], and lecithin:cholesterol acyltransferase [LCAT]) known to modify circulating plasma lipoproteins. Although the hepatic VLDL used for these studies were obtained from recirculating liver perfusions, Johnson, Swift, and Rudel (22) have shown that VLDL isolated from recirculating or nonrecirculating liver perfusion systems share the same particle morphology and composition. Hepatic VLDL resemble their plasma counterparts but are relatively less cholesteryl ester-enriched and have a higher percentage of phospholipid that may represent the excess surface material (see Fig. 1). These hepatic VLDL would have to undergo core and surface modifications to resemble LDL. These changes would include: *1*) loss of core TG; *2*) loss or gain of core CE, depending on the particle; and *3*) loss of surface material including apoE and apoC (19, 20, 22). It is conceivable that hepatic VLDL are preferred sub-

Downloaded from www.jlr.org by guest, on June 19, 2012

strates for lipoprotein lipase and are hydrolyzed rapidly, similar to that seen in chylomicron metabolism (48). The rapid conversion of hepatic VLDL to LDL in the current studies suggests that hepatic VLDL may also be efficient substrates for other intravascular enzymes such as hepatic lipase, LCAT, and/or LTP. Nascent hepatic VLDL, LDL, and HDL have been shown to be excellent substrates for LCAT (29, 49). Noel et al. (50) have shown that rat hepatic VLDL are better cholesteryl ester acceptors than are rat and human plasma VLDL, and proposed that this difference was due to the high TG:CE ratio of the hepatic VLDL compared to plasma VLDL. Relatively high TG:CE ratios are common among hepatic apoB-containing lipoproteins compared to their plasma equivalents (16–22). Together with the metabolic studies presented here, these data suggest that nascent hepatic lipoproteins may be superior substrates for intravascular enzymes compared to plasma lipoproteins because of their physical and chemical properties.

The design of these studies was unique. The use of DGUC to describe the movement of radioactivity into and out of various lipoprotein subfractions has provided additional information regarding lipoprotein metabolism. There are several advantages to using DGUC for metabolic studies. First, the distribution of lipoproteins throughout the density gradient defines the density ranges of the various subfractions that may exist in any given subject. This is important since the physical properties and characteristics of lipoproteins vary among individuals (9–11; Krauss, R. M., J. J. Albers, M. A. Austin, and J. D. Brunzell, unpublished observations). Second, DGUC techniques can further define precursor–product relationships among lipoprotein subfractions. For instance, DGUC can be used to help determine whether certain subpopulations of VLDL are metabolized to specific LDL subfractions. Finally, DGUC can help determine the distribution of various precursors in relationship to the mass distribution of plasma lipoproteins. However, as with other ultracentrifugation methods, the separation of various lipoprotein subfractions is incomplete and cross-contamination between density subpopulations no doubt exists. Additional analyses such as curve peeling might help in examining the distribution of lipoproteins across these density gradients.

The results from the present studies emphasize the complexities of the structural and kinetic heterogeneity within plasma LDL. The turnover rates differed between LDL_1 and LDL_2 as well as between hepatic lipoprotein-derived [^{3}H]LDL_1 and [^{3}H]LDL_2 and plasma-derived ^{125}I-labeled LDL_1 and ^{125}I-labeled LDL_2. In all animals, [^{3}H]LDL_1 had a higher turnover rate that did [^{3}H]LDL_2 (see Table 2). Metabolic heterogeneity within the LDL class has been described previously in nonhuman primates (28, 45) and in human subjects (4–7). In addition, the current studies have shown that in some animals the final slope of the hepatic lipoprotein-derived LDL_1 subfractions had slower turnover rates than their plasma LDL-derived counterparts (see Fig. 4). The different rates of decay between ^{3}H-labeled and ^{125}I-labeled LDL apoB-100 suggest at least two possibilities: *1*) that the recipient's own hepatic lipoproteins are different from the injected hepatic particles; and/or *2*) that these hepatic lipoproteins represent only a portion of the hepatic precursors that contribute to LDL, each of which has a different turnover rate after conversion to LDL. This latter hypothesis is supported by additional studies in which hepatic LDL isolated between d 1.030 and 1.063 g/ml were metabolically similar, but had different final rates of decay than their plasma LDL counterparts (51). Further kinetic analyses of plasma LDL ^{125}I-labeled apoB-100 are currently underway to complete the plasma LDL kinetic model and estimate the amount of LDL apoB-100 derived from hepatic VLDL versus the amount derived from other sources.

The animals used in these studies were fed cholesterol-containing diets with either 40% of total calories as saturated or polyunsaturated fat. Although total plasma cholesterol concentrations ranged from 160 to 590 mg/dl, African green monkeys, like human subjects, vary in their response to dietary cholesterol. In spite of the diversity in lipoprotein cholesterol concentrations or source of dietary fat among the animals, the metabolic behavior of the hepatic VLDL and plasma LDL was similar in all animals and shared the same kinetic characteristics as shown by the model. The potential analogies that can be drawn between lipoprotein metabolism in cholesterol-fed African green monkeys and human subjects remain unclear. However, these studies support earlier suggestions made in human subjects that a portion of LDL might be produced from the rapid conversion of a small pool of VLDL or IDL precursors (13–15). Evidence of this pathway existing in human subjects is difficult to obtain. Even in studies using [^{3}H]leucine (4), it is hard to distinguish between LDL synthesized directly by the liver from LDL produced from the rapid conversion of nascent precursor particles to LDL.

The authors would like to thank Ann Ferguson and Linda Odham for their skillful efforts in the preparation of this manuscript. This work was supported by National Institutes of Health Grants HL-14164, HL-30086, and RR-02176, and by a grant from the North Carolina Heart Association. CAM was partially supported by an Institutional National Research Service Award HL-07115 and partly as an R. J. Reynolds Industries Special Fellow. Portions of this work have been presented in abstract form in *Fed. Proc.* **44:** 8018 (1985) and *Arteriosclerosis.* **6:** 569a (1986).

Manuscript received 28 March 1988 and in revised form 27 July 1988.

Downloaded from www.jlr.org by guest, on June 19, 2012

REFERENCES

1. Krauss, R. M., and D. J. Burke. 1982. Identification of multiple subclasses of plasma low density lipoproteins in normal humans. *J. Lipid Res.* **23:** 97–104.
2. Shen, M. S. M., R. M. Krauss, F. T. Lindgren, and T. M. Forte. 1981. Heterogeneity of serum low density lipoproteins in normal subjects. *J. Lipid Res.* **22:** 236–244.
3. Nelson, C. A., and M. D. Morris. 1977. The ultracentrifugal heterogeneity of serum low density lipoproteins in normal humans. *Biochem. Med.* **18:** 1–9.
4. Fisher, W. R., L. A. Zech, P. Bardalye, G. Warmke, and M. Berman. 1980. Metabolism of apolipoprotein B in subjects with hypertriglyceridemia and polydisperse LDL. *J. Lipid Res.* **21:** 760–774.
5. Teng, B., A. D. Sniderman, A. K. Soutar, and G. R. Thompson. 1986. Metabolic basis of hyperapobetalipoproteinemia. Turnover of apolipoprotein B in low density lipoprotein and its precursors and subfractions compared with normal and familial hypercholesterolemia. *J. Clin. Invest.* **77:** 663–672.
6. Vega, G. L., and S. M. Grundy. 1986. Kinetic heterogeneity of low density lipoproteins in primary hypertriglyceridemia. *Arteriosclerosis.* **6:** 395–406.
7. Foster, D. M., A. Chait, J. A. Albers, R. A. Failor, C. Harris, and J. D. Brunzell. 1986. Evidence for kinetic heterogeneity among human low density lipoproteins. *Metabolism.* **35:** 685–696.
8. Teng, B., G. R. Thompson, A. D. Sniderman, T. M. Forte, R. M. Krauss, and P. O. Kwiterovich. 1983. Composition and distribution of low density lipoprotein fractions in hyperapobetalipoproteinemia, normolipoproteinemia, and familial hypercholesterolemia. *Proc. Natl. Acad. Sci. USA.* **80:** 6662–6666.
9. Marzetta, C. A., D. M. Foster, J. E. Hokanson, R. A. Failor, and J. D. Brunzell. 1987. LDL in familial combined hyperlipidemia and other hypertriglyceridemic states. *In* Proceedings of the Workshop on Lipoprotein Heterogeneity. K. Lippel, editor. NIH Publication No. 87-2646. 285–292.
10. Failor, R. A., J. E. Hokanson, and J. D. Brunzell. 1986. Low density lipoproteins in familial hyperlipidemias. *In* Atherosclerosis VII. N. H. Fidge and P. Nestel, editors. Excerpta Medica, New York. 159–163.
11. Crouse, J. R., J. S. Parks, H. M. Schey, and F. R. Kahl. 1985. Studies of low density lipoprotein molecular weight in human beings with coronary heart disease. *J. Lipid Res.* **26:** 566–574.
12. Kesaneimi, Y. A., G. L. Vega, and S. M. Grundy. 1982. Kinetics of apolipoprotein B in normal and hyperlipidemic man: Review of current data. *In* Lipoprotein Kinetics and Modeling. M. Berman, S. M. Grundy, and B. V. Howard, editors. Academic Press, San Francisco, CA. 181–205.
13. Beltz, W. F., Y. A. Kesaniemi, B. V. Howard, and S. M. Grundy. 1985. Development of an integrated model for analysis of the kinetics of apolipoprotein B in plasma very low density lipoproteins, intermediate density lipoproteins, and low density lipoproteins. *J. Clin. Invest.* **76:** 596–603.
14. Shepherd, J., and C. J. Packard. 1987. Metabolic heterogeneity in very low-density lipoproteins. *Am. Heart J.* **113:** 503–508.
15. Goldberg, I. J., N-A. Le, R. M. Krauss, and F. T. Lindgren. 1988. Lipoprotein metabolism during acute inhibition of lipoprotein lipase in the cynomolgus monkey. *J. Clin. Invest.* **81:** 561–568.
16. Marsh, J. B. 1974. Lipoproteins in a nonrecirculating perfusate of rat liver. *J. Lipid Res.* **15:** 544–550.
17. Noel, S-P., L. Wong, P. J. Dolphin, L. Dory, and D. Rubenstein. 1979. Secretion of cholesterol-rich lipoproteins by perfused livers of hypercholesterolemic rats. *J. Clin. Invest.* **64:** 674–683.
18. Hornick, C. A., T. Kita, R. L. Hamilton, J. P. Kane, and R. J. Havel. 1983. Secretion of lipoproteins from the liver of normal and Watanabe heritable hyperlipidemic rabbits. *Proc. Natl. Acad. Sci. USA.* **80:** 6096–6100.
19. Johnson, F. L., R. W. St. Clair, and L. L. Rudel. 1983. Studies on the production of low density lipoproteins by perfused livers from nonhuman primates. Effect of dietary cholesterol. *J. Clin. Invest.* **72:** 221–235.
20. Johnson, F. L., R. W. St. Clair, and L. L. Rudel. 1985. Effects of the degree of saturation of dietary fat on the hepatic production of lipoproteins in the African green monkey. *J. Lipid Res.* **26:** 403–417.
21. Jones, L. A., T. Teramoto, D. J. Juhn, R. B. Goldberg, A. H. Rubenstein, and G. S. Getz. 1984. Characterization of lipoprotein produced by the perfused rhesus monkey liver. *J. Lipid Res.* **25:** 319–335.
22. Johnson, F. L., L. L. Swift, and L. L. Rudel. 1987. Nascent lipoproteins from recirculating and nonrecirculating liver perfusions and from the hepatic Golgi apparatus of African green monkeys. *J. Lipid Res.* **28:** 549–564.
23. Teramoto, T., H. Kato, Y. Hashimoto, M. Kinoshita, T. Watanabe, H. Oka, and C. Naito. 1987. Effect of dietary cholesterol on production of lipoproteins and apolipoproteins by perfused livers from Japanese monkeys (*Macaca fuscata*). *Eur. J. Clin. Invest.* **17:** 522–529.
24. Thrift, R. N., T. M. Forte, B. E. Cahoon, and V. G. Shore. 1986. Characterization of lipoproteins produced by the human liver cell line, Hep G2, under defined conditions. *J. Lipid Res.* **27:** 236–250.
25. Ellsworth, J. L., S. K. Erikson, and A. D. Cooper. 1986. Very low and low density lipoprotein synthesis and secretion by the human hepatoma cell line Hep-G2: effects of free fatty acids. *J. Lipid Res.* **27:** 858–874.
26. Dashti, N., and G. Wolfbauer. 1987. Secretion of lipids, apolipoproteins, and lipoproteins by human hepatoma cell line, HepG2: effects of oleic acid and insulin. *J. Lipid Res.* **28:** 423–436.
27. Marzetta, C. A., and L. L. Rudel. 1986. A species comparison of low density lipoprotein heterogeneity in nonhuman primates fed atherogenic diets. *J. Lipid Res.* **27:** 753–762.
28. Melchior, G. W., and L. L. Rudel. 1978. Heterogeneity in the low density lipoproteins of cholesterol-fed African green monkeys (*Cercopithecus aethiops*). *Biochim. Biophys. Acta.* **531:** 331–343.
29. Babiak, J., H. Tamachi, F. L. Johnson, J. S. Parks, and L. L. Rudel. 1986. Lecithin:cholesterol acyltransferase-induced modifications of liver perfusate discoidal high density lipoproteins from African green monkeys. *J. Lipid Res.* **27:** 1304–1317.
30. Rudel, L. L., C. A. Marzetta, and F. L. Johnson. 1986. Separation and analysis of lipoproteins by gel filtration. *Methods Enzymol.* **129:** 45–57.
31. McFarlane, A. S. 1958. Efficient trace labeling of proteins with iodine. *Nature (London)* **182:** 53–57.
32. Bilheimer, D. W., S. Eisenberg, and R. I. Levy. 1972. The metabolism of very low density lipoprotein proteins. Preliminary in vitro and in vivo observations. *Biochim. Biophys. Acta.* **260:** 212–221.
33. Rudel, L. L., and M. D. Morris. 1973. Determination of

Downloaded from www.jlr.org by guest, on June 19, 2012

cholesterol using *o*-phthalaldehyde. *J. Lipid Res.* **14:** 364–366.
34. Sardesai, V. M., and J. A. Manning. 1968. The determination of triglyceride in plasma and tissues. *Clin. Chem.* **14:** 156–161.
35. Lowry, O. H., N. J. Rosebrough, A. L. Farr, and R. J. Randall. 1951. Protein measurement with the Folin phenol reagent. *J. Biol. Chem.* **193:** 265–275.
36. Berman, M., and M. F. Weiss. 1978. SAAM Manual. DHEW Publication (NIH) 78–180.
37. Berman, M., W. F. Beltz, P. C. Grief, R. Chabay, and R. C. Boston. 1983. CONSAM User's Guide. U.S. Department of Health and Human Services, NIH.
38. Snedecor, G. W., and W. G. Cochran. 1974. Statistical Methods. Iowa State University Press. Ames, Iowa.
39. Goldberg, I. J., N-A. Le, H. N. Ginsberg, J. R. Paterniti, and W. V. Brown. 1983. Metabolism of apoB in cynomolgus monkey: evidence for independent production of low density lipoprotein apoB. *Am. J. Physiol.* **244:** E196–E201.
40. Janus, E. D., A. Nicoll, R. Wootton, P. R. Turner, P. J. Magill, and B. Lewis. 1980. Quantitative studies of very low density lipoproteins: conversion to low density lipoproteins in normal controls and primary hyperlipidaemic states and the role of direct secretion of low density lipoproteins in heterozygous familial hypercholesterolemia. *Eur. J. Clin. Invest.* **10:** 149–159.
41. Kesanemi, Y. A., W. F. Beltz, and S. M. Grundy. 1985. Comparisons of metabolism of apolipoprotein B in normal subjects, obese patients, and patients with coronary heart disease. *J. Clin. Invest.* **76:** 586–595.
42. Soutar, A. K., N. B. Myant, and G. R. Thompson. 1977. Simultaneous measurement of apolipoprotein B turnover in very-low and low-density lipoproteins in familial hypercholesterolaemia. *Atherosclerosis.* **28:** 247–256.
43. Ginsberg, H. N., N-A. Le, and J. C. Gibson. 1985. Regulation of the production and catabolism of plasma low density lipoproteins in hypertriglyceridemic subjects. *J. Clin. Invest.* **75:** 614–623.
44. Illingworth, D. R. 1975. Metabolism of lipoproteins in non-human primates. Studies on the origin of low density lipoprotein in the plasma of the squirrel monkey. *Biochim. Biophys. Acta.* **388:** 38–57.
45. Goldberg, I. J., N-A. Le, B. Leeman, W. V. Brown, and F. T. Lindgren. 1986. Evidence for heterogeneity of low density lipoprotein metabolism in the cynomolgus monkey. *Biochim. Biophys. Acta.* **879:** 179–185.
46. Huff, M. W., and D. E. Telford. 1985. Direct synthesis of low-density lipoproteins in the miniature pig. *Metabolism.* **34:** 36–42.
47. Fidge, N. H., and P. Poulis. 1978. Metabolic heterogeneity in the formation of low density lipoprotein from very low density lipoprotein in the rat: evidence for the independent production of a low density lipoprotein subfraction. *J. Lipid Res.* 1978. **19:** 342–349.
48. Grundy, S. M., and H. Y. I. Mok. 1976. Chylomicron clearance in normal and hyperlipidemic man. *Metabolism.* **25:** 1225–1239.
49. Hamilton, R. L., M. C. Williams, C. J. Fielding, and R. J. Havel. 1976. Discoidal bilayer structure of nascent high density lipoproteins from perfused rat liver. *J. Clin. Invest.* **58:** 667–680.
50. Noel, S-P., R. Duproas, C. Vezina, and Y. L. Marcel. 1984. Comparison of very-low-density lipoproteins isolated from rat liver perfusate, rat serum and human plasma as acceptors for cholesteryl ester transfer. *Biochim. Biophys. Acta.* **796:** 277–284.
51. Murthy, V. M., C. A. Marzetta, L. L. Rudel, L. A. Zech, and D. M. Foster. 1988. The contribution of particles of hepatic origin to plasma LDL in African green monkeys. *FASEB J.* **2:** 1039 (abstract).

Downloaded from www.jlr.org by guest, on June 19, 2012